Available online at www.sciencedirect.com
ScienceDirect
Applied Geochemistry 22 (2007) 109–127
Applied Geochemistry
www.elsevier.com/locate/apgeochem

Solid-phase control on the mobility of potentially toxic elements in an abandoned lead/zinc mine tailings impoundment, Taxco, Mexico

F.M. Romero [a], M.A. Armienta [b,*], G. González-Hernández [b]

[a] *Instituto de Geografía, Universidad Nacional Autónoma de México, UNAM, CU, México 04510 D.F., Mexico*
[b] *Instituto de Geofísica, Universidad Nacional Autónoma de México, UNAM, CU, México 04510 D.F., Mexico*

Received 25 October 2005; accepted 28 July 2006
Editorial handling by J. Webster-Brown
Available online 1 November 2006

Abstract

Detailed mineralogical and geochemical investigations were conducted within abandoned Pb and Zn flotation tailings at "El Fraile" impoundments in Taxco, Guerrero, central-southern México. These tailings are divided into an active oxidation zone near the surface, an underlying transition zone and an unoxidized zone. Although these tailings have undergone 30 a of sulfide oxidation, the active oxidation zone has only penetrated to a depth of 0.2 m in the settling pond, and to 0.6–1.2 m in the dam. The oxidation of sulfide minerals and the insufficiency of pH-buffering minerals have produced low-pH conditions (pH = 1.9–4.4) and high concentrations of dissolved SO_4^{2-}, As and heavy metals: SO_4^{2-} (1534–10086 mg L^{-1}), Fe (1.5–2568 mg L^{-1}), Zn (36.7–2435 mg L^{-1}), Cd (0.4–30.6 mg L^{-1}), Pb (<0.01–0.6 mg L^{-1}), Cu (0.5–38.2 mg L^{-1}) and As (0.01–164 mg L^{-1}). These concentrations of dissolved constituents are attenuated by a series of precipitation and sorption reactions. Precipitation of secondary phases, gypsum, goethite, hematite and K-jarosite has led to the formation of cemented layers within the active oxidation zone in the tailings dam. These cemented layers act as a trap for released, potentially toxic elements from the overlying oxidized tailings. Adsorption and coprecipitation on Fe-precipitates play an important role in the mobilization and attenuation of Zn, Cd, Cu and As within the "El Fraile" tailings. Additionally to the well-known ability of Fe-precipitates to strongly trap As and heavy metals, this study shows that precipitation of beudantite ($PbFe_3AsO_4SO_4(OH)_6$) appears to be one of the solid-phase controls on the natural attenuation of As and Pb and other heavy metals in these tailings.

1. Introduction

Historically, mining activities have produced vast quantities of inactive sulfide-bearing mine tailings in several regions of Mexico and throughout the world. These inactive tailings constitute potential environmental pollution sources due to the oxidation of sulfide minerals, which may result in the generation of acidic mine drainage (AMD), usually containing high concentrations of dissolved potentially toxic elements (PTE) and SO_4^{2-}. However, in mine tailings, acid-generating minerals (sulfide minerals) often

* Corresponding author.
E-mail address: victoria@geofisica.unam.mx (M.A. Armienta).

0883-2927/$ - see front matter © 2006 Elsevier Ltd. All rights reserved.
doi:10.1016/j.apgeochem.2006.07.017

occur in close association with acid-neutralizing minerals such as calcite and aluminosilicates. When sufficient acid-neutralizing minerals are present, the acid generated by sulfide oxidation is balanced by acid consumption and consequently, dissolved concentrations of PTE in tailings leachates and pore waters are relatively low (Blowes et al., 1998; Lin, 1997).

AMD has been recognized as the main environmental problem derived from mining activities (Dold and Fontbote, 2001; Holmstrom et al., 2001). The released PTE may be transported to the surrounding environment and contaminate soils, sediments, ground and surface waters (Armienta et al., 2001; Bain et al., 2000; Jung, 2001), thereby affecting the entire ecosystem. However, high concentrations of dissolved potentially toxic elements in AMD may be attenuated by a series of pH-buffering, precipitation and sorption reactions. Secondary minerals that precipitate during the oxidation-neutralization reactions can permanently or temporarily sequester PTE (Holmstrom and Ohlander, 2001; Levy et al., 1997). The secondary minerals more commonly reported in mine tailings are Fe-oxyhydroxides, jarosite and clay minerals, which function as a trap for released PTE through sorption processes.

Many authors have reported that these secondary Fe-precipitates and clay minerals have a large capacity for adsorption and coprecipitation of As and heavy metals. Consequently they are considered the main solid-phases' control on the mobility of potentially toxic elements in mine tailings (Courtin-Nomade et al., 2003; Dold and Fontbote, 2001; Foster et al., 1998; Fukushi et al., 2003; Holmstrom and Ohlander, 2001; Levy et al., 1997; Lin, 1997; Ljungberg and Ohlander, 2001; McGregor et al., 1998; Moncur et al., 2005; Savage et al., 2000). In addition, the occurrence of secondary scorodite has been identified in mine tailings (Foster et al., 1998; Paktunc et al., 2004; Roussel et al., 2000). Nevertheless, scorodite is not a relevant candidate for As immobilization *in situ*, due to the high pH dependence of its solubility and to high As concentrations at equilibrium (Roussel et al., 2000). Finally, a few authors have reported that precipitation of secondary beudantite may play an important role on the natural attenuation of As and Pb in mine tailings (Courtin-Nomade et al., 2002; Roussel et al., 2000).

Precipitation of secondary minerals within shallow zones of inactive sulfide tailings additionally causes the formation of cemented layers (Blowes et al., 1991; Courtin-Nomade et al., 2003; McGregor and Blowes, 2002). According to these authors, the cement layers act as an accumulation zone that retains PTE in the tailings and thereby moderates the severity of their environmental effects. Secondary minerals precipitated in acid mine environments may be the dominant sink for released PTE and therefore, from a remediation standpoint act as a natural attenuator of these elements. In this respect, secondary minerals may be preferable to engineered containment methods (Levy et al., 1997).

To develop an effective management strategy for AMD, it is necessary to understand the geochemical processes occurring in the tailings to identify the solid-phase controls on the mobilization and attenuation of PTE. However, the identification of these solid phases in bulk tailings samples (using X-ray diffraction and microscopy) is extremely difficult, because -within flotation sulfide tailings-, more than 80% of the concentration of PTE is contained in the finest particles (<40 μm) (IMMSA, 1980). A detailed geochemical investigation was conducted to assess a tailings remediation program at "El Fraile" inactive sulfide-rich impoundment in Taxco, Mexico. The objectives of this study were: (i) to evaluate the extent of sulfide oxidation within the tailings impoundment and subsequent release of the oxidation products, (ii) to evaluate the potential for the development of acidic drainage (iii) to identify the solid-phase controls on the mobility of sulfide-bound elements, in particular that of Pb, Zn, Cd, Cu and As.

2. Study site

The flotation treatment plant "El Fraile" started operations in 1945 and finished them around 1973. The average composition of the processed sulfide ore was 160 g t^{-1} Ag, 3.6% Pb and 7.6% Zn. In this period, 5.4×10^6 tons of sulfide mine tailings were generated and discharged in two adjacent narrow valleys. The tailings were deposited on calcareous shale of the Mexcala formation resulting in tailings impoundments "A" and "B", covering an area of 20 ha in the Taxco region, located in south-central México (Fig. 1).

The disposal technique at "El Fraile" caused hydraulic sorting of the tailings particles, resulting in the formation of a shallow, basin-shaped deposit of smaller particles (settling pond) and a high containment dyke of coarser particles (dam). In 1974,

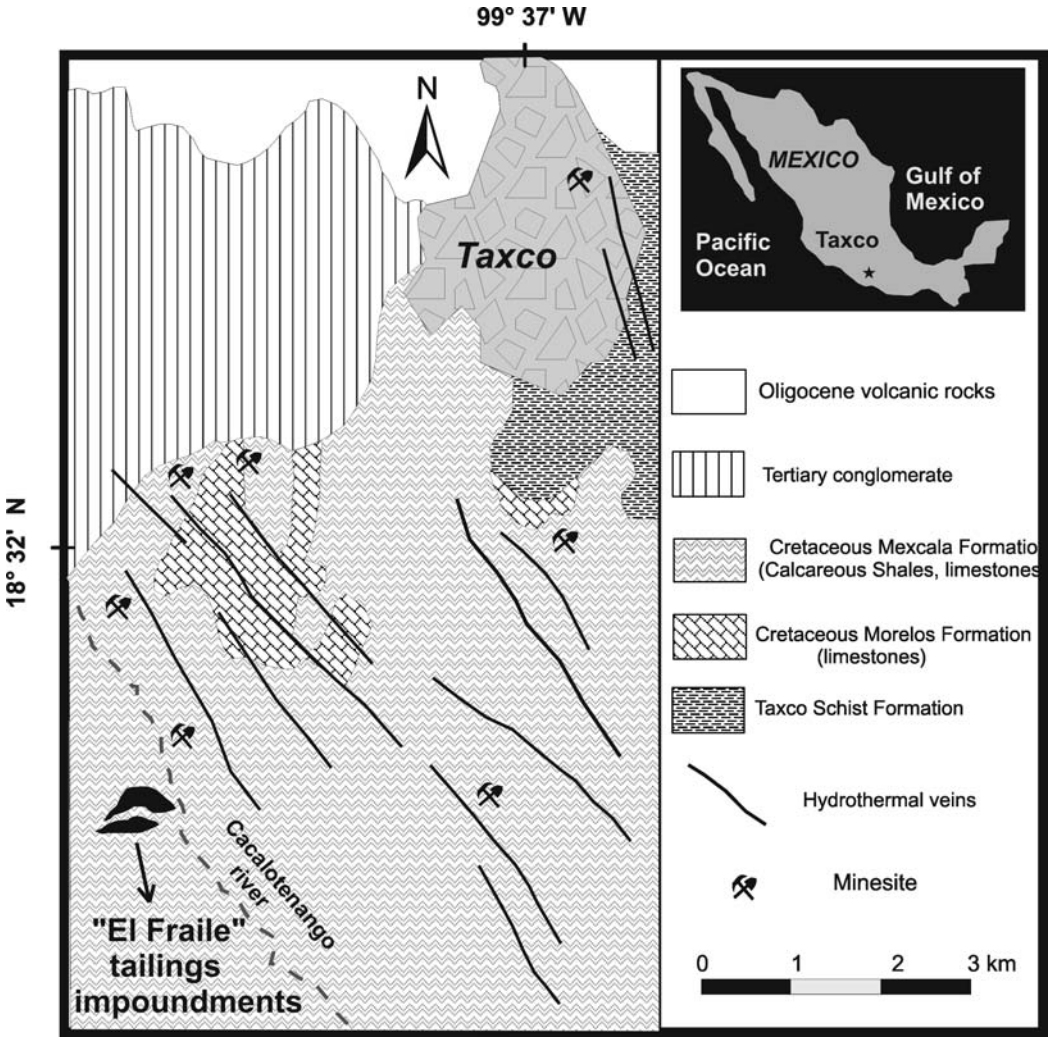

Fig. 1. Geological map showing the location of the "El Fraile" tailings impoundments.

the tailings deposited in the settling pond were covered with calcareous shale, and today this part of the tailings is totally vegetated and integrated to the natural landscape. At present, only the tailings dam remains exposed (Fig. 2).

The Taxco mining area has been one of the most important producers of base and precious metals since pre-Hispanic times. Mineralization appears mainly in hydrothermal veins, replacement ores and stockworks hosted in limestone, shale and schist (Fig. 1). The main sulfide minerals in the area are pyrite (10–15%), sphalerite (11%) and galena (4%). Among the main gangue minerals, quartz, calcite and feldspar have been reported (IMMSA, 1973). Other primary sulfide minerals in veins throughout the Taxco area are chalcopyrite, argentite, pirargite, proustite and arsenopyrite. The ore also contains minor quantities of goethite, hematite, cerusite, anglesite, melanterite and barite. This mining area is located at an altitude of 1700 masl.

The climate of the region is warm and sub-humid with an annual average temperature of 26–30 °C with a minimum of 12 °C and a maximum of 35 °C. The historical precipitation registry indicates an annual average of the order of 1000 mm (INEGI, 1999). However, this precipitation concentrates from June to October with maximum values in September (300 mm). Maximum temperatures of 35 °C are registered in these months favoring evapo-transpiration. From December to May the precipitations are scarce with minimum values in February (1.2 mm). These weather conditions have led to

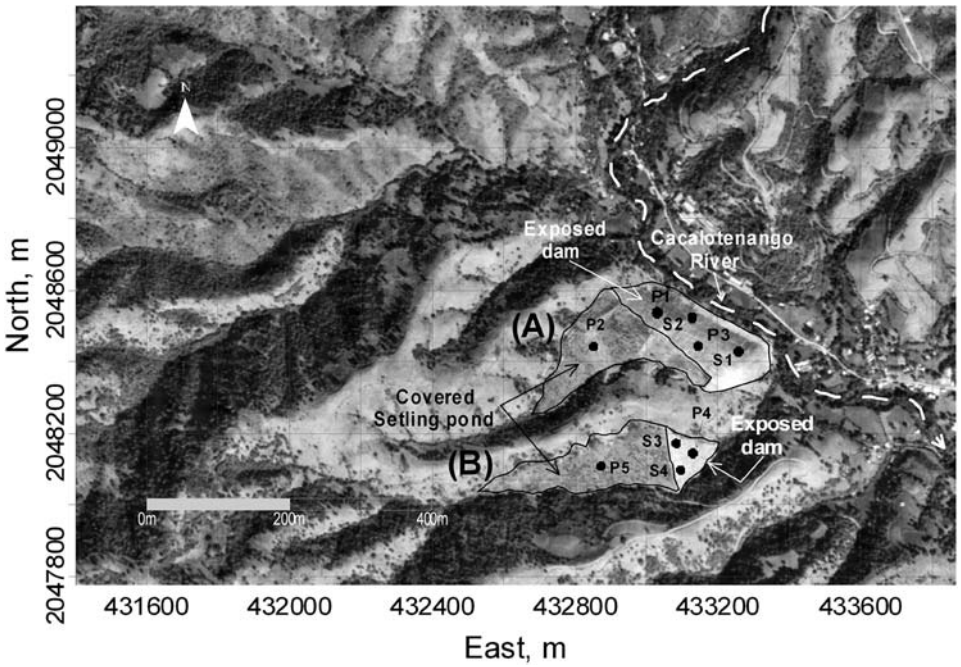

Fig. 2. Sampling location of tailings at "El Fraile" impoundments "A" and "B" S1, S2, S3, S4 correspond to excavation pits of 50 cm depth and and P1, P2, P3, P4, P5 correspond to excavation pits of 200 cm depth.

water level depths deeper than 2 m within the tailing piles.

3. Methods

A total of 37 solid samples were collected in excavation pits of 50 and 200 cm depth (Fig. 2). The sampling sites were selected according to the heterogeneity of tailings taking into account color, texture, degree of concretion and pH measured in field. According to visual characteristics, sampling intervals at each core varied between 10 and 30 cm. The solid samples were stored in hermetically sealed plastic bags to minimize dust contamination during transport to the laboratory. Samples were air dried, disaggregated and homogenized.

Total concentration of major elements was determined using X-ray fluorescence spectrometry (XRF) with a sequential XRF Spectrometer (SIEMENS SRS 3000). The potentially toxic elements were analyzed with Inductively Coupled Plasma Atomic Emission Spectroscopy (ICP-AES) according to the EPA 6010 A method (USEPA, 1996), after microwave assisted acid digestion following the USEPA 3051 procedure (USEPA, 1994).

All samples were analyzed as bulk samples by X-ray diffraction (XRD) using a SIEMENS D5000 difractometer (Cu Kα radiation, $\lambda = 1.5406$ Å). Polished thin sections from 12 representative samples were prepared and analyzed by optical and scanning electron microscopy with energy dispersive X-ray spectrometry (SEM-EDS). SEM-EDS analyses were done using a JEOL JXA-8900R superprobe.

Samples were also sieved through U.S. Standard Sieves with the purpose of concentrating particles smaller than 40 μm, which retain most of the PTE (IMMSA, 1980). Concentrated samples were analyzed by XRD and SEM-EDS. A transmission electron microscopy (TEM) analysis of Pb-As-rich particles was done on a JEOL 2010 FEG transmission electron microscope, working at 200 kV and a resolution of 1.7 Å. The selected area aperture to obtain electron-diffraction patterns was approximately 10 μm in diameter. Sample powder was dispersed in ethanol and deposited on Cu mesh grids, previously covered by a graphite film. This technique allows a direct identification of the minerals containing the PTE, generally in low concentrations in mine tailings, and therefore not easily detected by conventional techniques. TEM electronic diffraction patterns provide the crystalline structure of the particles that contain the PTE of interest enabling the recognition of the specific PTE mineral.

Paste pH was determined by weighing 20 g of air-dried sample and adding 20 mL of distilled water. After mixing for 5 s the slurry was left to stand

for 10 min. The electrodes were then inserted in the slurry and after swirling slightly the pH was measured until a constant value was obtained.

Since climatic conditions did not allow the extraction of pore tailings solution in the field, in order to evaluate the chemistry of aqueous tailings leachates a 50-g homogenized sample was suspended in 150 mL de-ionized water in plastic bottles. Sample suspensions were agitated on a rotary shaker at 120 rpm until the stabilization of pH and electric conductivity (EC) was obtained (8 days). This method has been successfully used by Martycak et al. (1994) in samples of ore deposits, as well as Lin (1997) in tailing's samples. The method is based on the presumption that leachates are developed from primarily dilute pore solutions which interact with the disintegrated solids. The complete transition of the pore solution into leachates is indicated by the pH stabilization of the extractant (Martycak et al., 1994). These leachates were used to approximate the tailings pore solution. After pH and EC stabilization, leachates were decanted and filtered through a 0.45 μm Millipore filter.

Each clear aqueous extract was divided into two subsamples. One was acidified with $HNO_3$to preserve metal concentration, and the other was left unacidified. Unacidified extracts were analyzed for pH, redox potential, carbonate species, SO_4^{2-}, and Cl^-. Acidified extracts were analyzed for Ca, Mg, Mn, Al, Na, K, Fe, Zn, Cd, Pb, Cu and As using ICP-AES. Carbonate and HCO_3^- were measured by acid titration. Sulfate was determined by turbidimetry through the formation of Ba SO_4 by adding $BaCl_2$. Chloride was determined by potentiometry using an ion selective electrode. Redox potential was measured with an Ag/AgCl electrode. Analytical data quality was controlled through the analyses of all samples in duplicate, and of blanks and reference materials (Sulfide ore mill tailing RTS-3 Canadian standard). Analysis of duplicate samples indicated 10% reproducibility. Accuracy was within 90–115%. Charge imbalance calculations in the aqueous extracts were below 8%.

Chemical modeling of the aqueous extracts was performed using the MINTEQA2 (Allison et al., 1991) computer code. MINTEQA2 is an equilibrium speciation model that uses a pre-defined set of components including free ions and neutral and charged complexes. The data base of reactions is written in terms of these components as reactants. The program solves the multiple-component chemical equilibrium by the simultaneous solution of the nonlinear mass action expressions and linear mass balance relationships. Concentrations determined in the leachates were used to calculate the ionic strength by the model. Activity coefficients were calculated with the Davies equation. Initial activity guesses for the input components are provided in the input file for a given problem in the MINTEQA2 program. Successive sets of activity coefficients are calculated for all solution species at each iteration. Each iteration improves the estimation of species concentrations and activity corrections. MINTEQA2 terminates the calculations if the charge balance exceeds 10%. Saturation indexes were computed with the model considering a temperature of 25 °C. Ksp values were taken from the database of the geochemical program.

4. Results and discussion

4.1. Zoning characterization

The tailings at "El Fraile" impoundments "A" and "B" have been subjected to supergene alteration, which has led to a characteristic zoning. However, different degrees of exposure between the dam and settling pond have led to different degrees of alteration. The tailings dam has been exposed to oxidizing agents during 30 a. On the other hand, the settling pond was covered with a layer of calcareous shale immediately after the end of mining operations. The alteration process has consequently been more intensive in the tailings dam in relation to the settling pond. In cross-section, 3 main geochemical zones can be distinguished in impoundments "A" and "B". These zones are distinctive in color, cementation, pH values and mineral content and comprise, from bottom to top: an unoxidized zone, a transition zone, and an active oxidation zone.

4.1.1. Unoxidized and transition zones

The unoxidized zone is composed of friable and dark gray tailings with near neutral paste pH values (pH = 6.5–7.2). This zone occurs at depths between 65 cm and 120 cm below the tailings surface in the dam and in the settling pond (Fig. 3). The transition zone overlies unoxidized tailings and consists of friable tailings of gray–green color with near neutral paste pH values (6.0–7.0). The thickness of the transition zone varies between 15 and 80 cm.

XRD and microscopic studies in bulk samples from the dam and settling pond showed that in

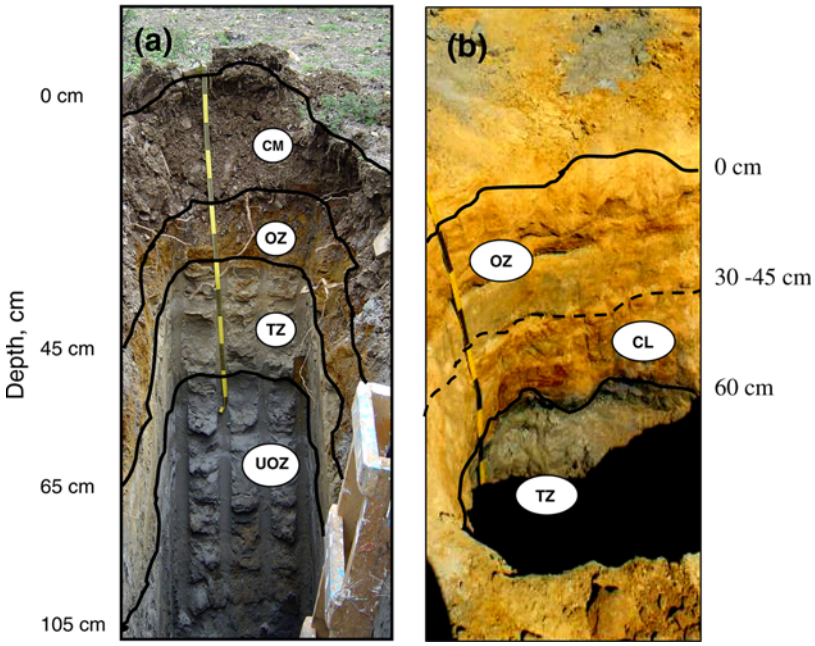

Fig. 3. Representative profiles through the "El Fraile" tailings: (a) in the settling pond, and (b) in the dam. CM: cover material, OZ: oxidation zone, CL: cemented layer, TZ: transition zones, UOZ: unoxidized zone.

the unoxidized and transition zones the original sulfide assemblage is dominated by pyrite and sphalerite. Results of SEM-EDS analysis showed that some pyrite and sphalerite grains contain traces of As and Cd respectively. These sulfide minerals show no sign of weathering in the unoxidized zone while the tailings in the transition zone are weakly altered. The approximate relative abundance of sulfide minerals, which was determined by point-counting in the polished sections, indicates that unoxidized tailings contain approximately 10% pyrite, 4% sphalerite and only traces of chalcopyrite and galena. Among the pH-buffering minerals, only aluminosilicate minerals were identified (plagioclase, orthoclase, epidote, ilvaite, muscovite and chlorite). Mineralogical analyses did not identify any discrete carbonate minerals, probably due to their relatively low abundances. SEM-EDS and optical microscopy analysis showed some grains of goethite, limonite, hematite and cerusite. These secondary phases in the unoxidized tailings are interpreted as a product of the supergene alteration of Pb–Zn ore, from which these tailings were derived.

4.1.2. Oxidized zone

The uppermost part of "El Fraile" tailings impoundment is an oxidation zone, both in the dam and in the settling pond and it is composed of tailings of yellow – brown color (Fig. 3). The oxidation zone in the dam starts at the tailings surface and reaches 65–120 cm depth. In general, near the surface, the oxidation zone consists of weakly cemented tailing layers that are mainly brownish yellow with a low paste pH (pH = 2.0–2.5). Towards the bottom, the tailings are lithified and cemented by brownish and reddish yellow precipitates, wherein paste pH values increase to 3.4–4.6. These cemented layers occur at depths between 20 and 50 cm below the surface, their total thickness varies from 15 cm to 80 cm.

The active oxidation zone in the settling pond consists of friable and brownish yellow tailings (uncemented) with low paste pH values (pH = 2.8–4.1). They are overlain by about 45 cm of calcareous shale used as cover material during remediation. The oxidation zone in the tailings settling pond has little development (thickness = 10–20 cm) in relation to the dam (Fig. 3). This may have resulted from the presence of the cover material as well as from a finer sized fraction of the tailings deposits that have restricted the oxidizing agent's diffusion through the settling pond, leading to a less extensive sulfide oxidation.

XRD and microscopic studies of bulk oxidized samples showed that the primary non-metallic minerals are dominated by quartz, orthoclase and

muscovite. Sulfide and carbonate minerals were not observed. Oxidation and acid-neutralization reactions have depleted the pyrite, sphalerite, plagioclase and chlorite content in oxidized tailings, allowing the formation of secondary minerals. XRD analysis showed that the secondary mineralogy of bulk oxidized tailings is dominated by gypsum, kaolinite, K-jarosite, lepidocrocite, goethite and hematite. The study of polished sections showed that sulfide oxidation was complete in the oxidized tailings dam and sulfide minerals were totally replaced by secondary Fe solid phases. Nevertheless, pyrite grains were found to be coated by Fe oxyhydroxides in some oxidized uncemented tailings within the settling pond.

4.2. Sulfide oxidation, acid generation and release of potentially toxic elements

Sulfide oxidation has been extensively reviewed in the literature and it is generally accepted that pyrite (FeS_2) oxidation is the main acid generating source (Balistrieri et al., 1999; Dold and Fontbote, 2001). Pyrite oxidation generates acid, SO_4^{2-} and Fe. Nevertheless, the oxidation of other sulfide minerals, such as sphalerite (ZnS), galena (PbS) and chalcopyrite ($CuFeS_2$), may release metal ions (Zn, Fe, Cu and Pb) but may not generate acidity (Balistrieri et al., 1999).

Oxidation of pyrite, the predominant sulfide mineral within the "El Fraile" tailings and insufficiency of pH-buffering minerals have produced low pH leachates in the oxidized zone. The acidic leachates contain high concentrations of SO_4^{2-}, heavy metals and As. These elements were released by the oxidation of pyrite and the other sulfide minerals identified. In general, the highest concentrations of dissolved constituents coincide with the lowest pH values in the leachates. Table 1 shows the ranges and average concentrations of dissolved constituents in oxidized tailings leachates, subdivided by their different pH values. The pH values and content of dissolved constituents form a stepwise profile in the tailings. Data from representative profiles from the tailings dam are shown in Fig. 4, and from the tailings settling pond in Fig. 5.

Near the surface of the oxidized tailings dam the leachate pH values are low (pH = 1.9–2.7). These low pH values rise gradually (pH = 3.5–4.4) where the underlying cemented layer is first met, which indicates that generated H^+ ions are consumed by dissolution of the identified aluminosilicate minerals. The highest concentrations of dissolved constituents were registered in these acidic and mildly acidic leachates of tailings from the oxidized zone (Table 1, Fig. 4). Below the cemented layer, wherein weakly altered and unoxidized tailings occur, the pH increases abruptly to near neutral (pH = 6.4–6.9) and dissolved concentrations of most metals and SO_4^{-2} decrease (Fig. 4). These results suggest that the cemented layer in the tailings dam has restricted the oxidizing agent's diffusion through them and has reduced the transport of dissolved constituents from the oxidized to the transition zone.

Sulfide oxidation of tailings from the settling pond, has resulted in the generation of mildly acidic leachates (pH = 2.9–4.0) in the oxidized zone. These pH values increase to near neutral (pH = 6.5) with depth, wherein the weakly altered tailings of the transition zone occur. The leachate pH values in the oxidized zone of the settling pond are higher in relation to those registered in leachates of the oxidized tailings dam and consequently, dissolved concentrations of constituents are lower. These results also suggest that sulfide oxidation has been less extensive in the settling pond, because the cover material has restricted the oxidizing agent's diffusion into the underlying zone. Nevertheless, the highest concentrations of most dissolved constituents were registered in leachates from transition zones in the settling pond (Fig. 5), suggesting that the absence of the cemented layer in the oxidized zone of the settling pond has allowed the transport of dissolved constituents from the oxidized to the transition zone. Below this zone, wherein unoxidized tailings occur, the leachate pH values are neutral (pH = 7.1) and most dissolved constituents show a sharp concentration decrease (Fig. 5).

Dissolution of secondary phases identified in the unoxidized tailings dam and settling pond associated to the supergene alteration of the Pb–Zn primary ore, may be the main source of the relatively low concentrations of dissolved SO_4^{2-} and PTE in the unoxidized tailings leachates. Additionally, dissolved SO_4^{2-} and Zn may be related to the reactants used in the flotation process.

On the other hand, sulfide oxidation reactions in the "El Fraile" tailings have depleted sulfide bound metals in the oxidized zone (Figs. 4 and 5). Table 2 shows that total concentrations of Fe, Cu, Zn and Cd are lower in the oxidized than in the unoxidized zones. The average bulk concentration of Fe (expressed as oxides) decreases from 15.6 wt.% in

Table 1
Ranges and average concentrations of dissolved constituents in oxidized tailings leachates

Constituent	Oxidized tailings leachates in tailings dam							Oxidized tailings leachates in settling pond	
	Uncemented layer				Cemented layer			Uncemented layer	
	"A"		"B"		"A"		"B"	"A"	"B"
	Range	Average ± SD	Range	Average ± SD	Range	Average ± SD	(*)	(*)	(*)
mg L^{-1}	pH = 2.3–2.7	pH = 2.5 ± 0.2	pH = 1.9–2.0	pH = 2.0 ± 0.1	pH = 4.1–4.4	pH = 4.3 ± 0.2	pH = 3.5	pH = 2.9	pH = 4.0
Al	35.4–326	166 ± 117	277–370	324 ± 65.8	12.8–182	97.4 ± 120	337	44.3	8.4
Ca	437–492	457 ± 20.6	433–442	438 ± 6.4	411–436	424 ± 17.7	395	492	509
K	0.1–1.3	0.6 ± 0.5	0.6–1.3	1 ± 0.5	1.5–1.8	1.7 ± 0.2	0.6	0.7	1.2
Mn	31.2–328	140 ± 101	57.9–69	63.5 ± 7.8	397–600	498 ± 144	421	9.6	16.9
Mg	14.7–238	106 ± 78.6	108–123	116 ± 10.6	147–350	249 ± 144	257	35	20.8
Na	0.2–1.5	0.8 ± 0.4	0.7–1.9	1.3 ± 0.8	0.8–1.6	1.2 ± 0.6	1.3	0.7	0.9
SO_4^{2-}	2278–6853	4354 ± 1728	8237–10086	9161 ± 1307	3715–6731	5223 ± 2133	8541	2047	1534
Fe	29–631	272 ± 237	2288–2568	2428 ± 198	1.5–6.8	4.1 ± 3.7	659	5.8	1.5
Zn	107–1309	514 ± 435	397–432	414 ± 25.2	645–2435	1540 ± 1265	2415	50.4	36.7
Pb	<0.01–0.1	0.04 ± 0.05	<0.01	<0.01	0.1–0.6	0.4 ± 0.4	<0.01	<0.01	0.1
Cu	2.1–18	10.2 ± 6.3	15.6–18.3	16.9 ± 2	0.5–4.7	2.6 ± 2.9	38.2	2.2	1.1
As	0.01–4	0.7 ± 1.6	101–164	133 ± 44.5	0.04–0.1	0.07 ± 0.02	0.4	0.1	0.02
Cd	1.1–18.2	6.7 ± 6.2	4.2–4.5	4.4 ± 0.2	3.6–25	14.4 ± 15.1	30.6	0.6	0.4

Note: (*) results of a single sample.

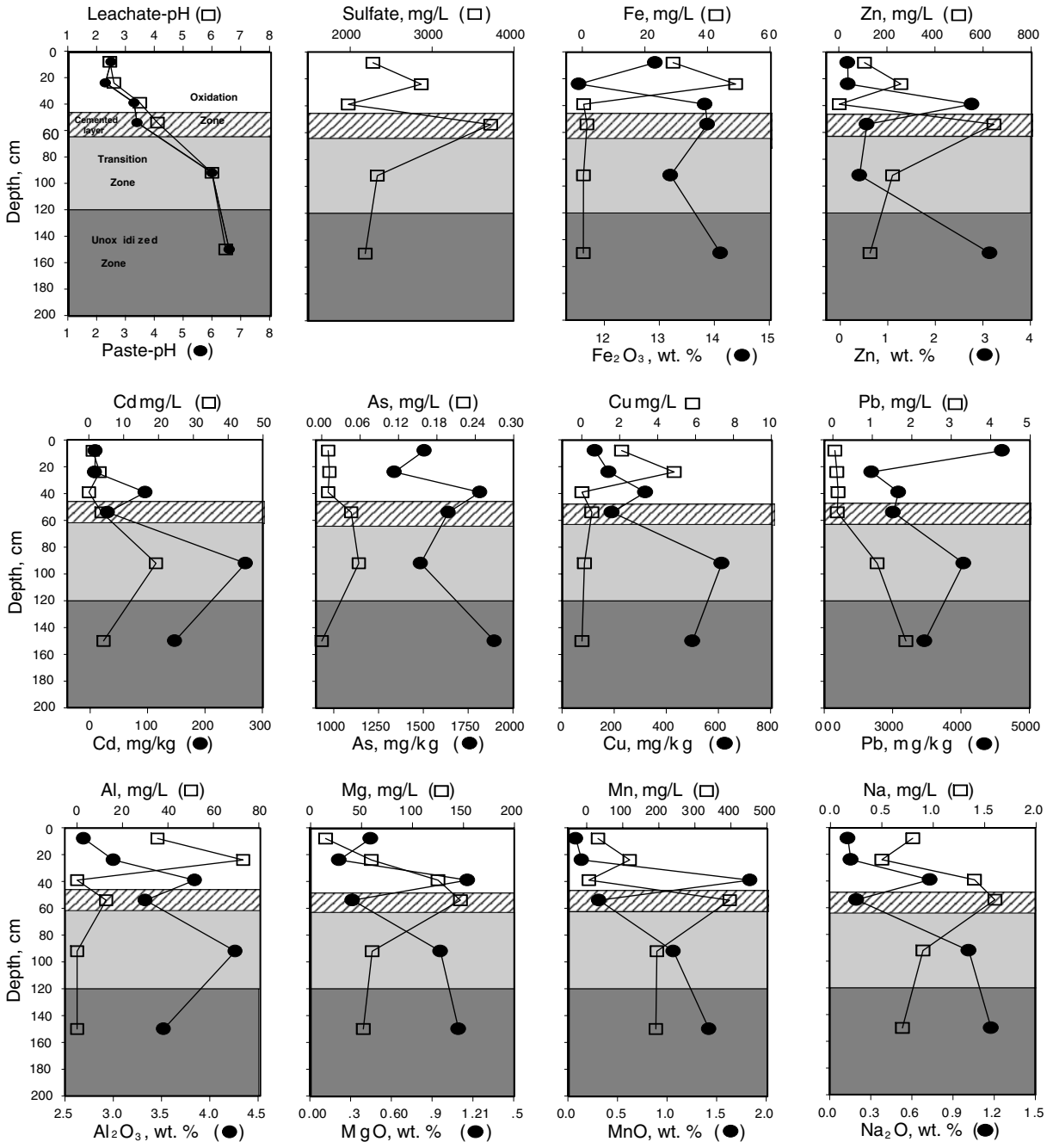

Fig. 4. Chemical composition of tailings solid samples (●) and leachates (□) from representative profile from tailings dam.

the unoxidized tailings to 11.2 wt.% in the oxidized tailings. Similarly, Zn concentration decreases from 25267 to 6079 mg kg^{-1}, Cd decreases from 186 to 33 mg kg^{-1} and Cu decreases from 340 to 199 mg kg^{-1}. The H^+ generated during pyrite oxidation, has favoured the incongruent dissolution of the aluminosilicate minerals that were identified (plagioclase, epidote, ilvaite, muscovite and chlorite) and consequently, the release of Al, Mn, Mg and Na into tailings leachates (Table 1). Aluminosilicate dissolution is indicated by depletion of the main aluminosilicate-bound elements Al, Mn, Mg, and Na. The bulk concentration of Al (expressed as oxides) decreases from an average of 4.7 wt.%

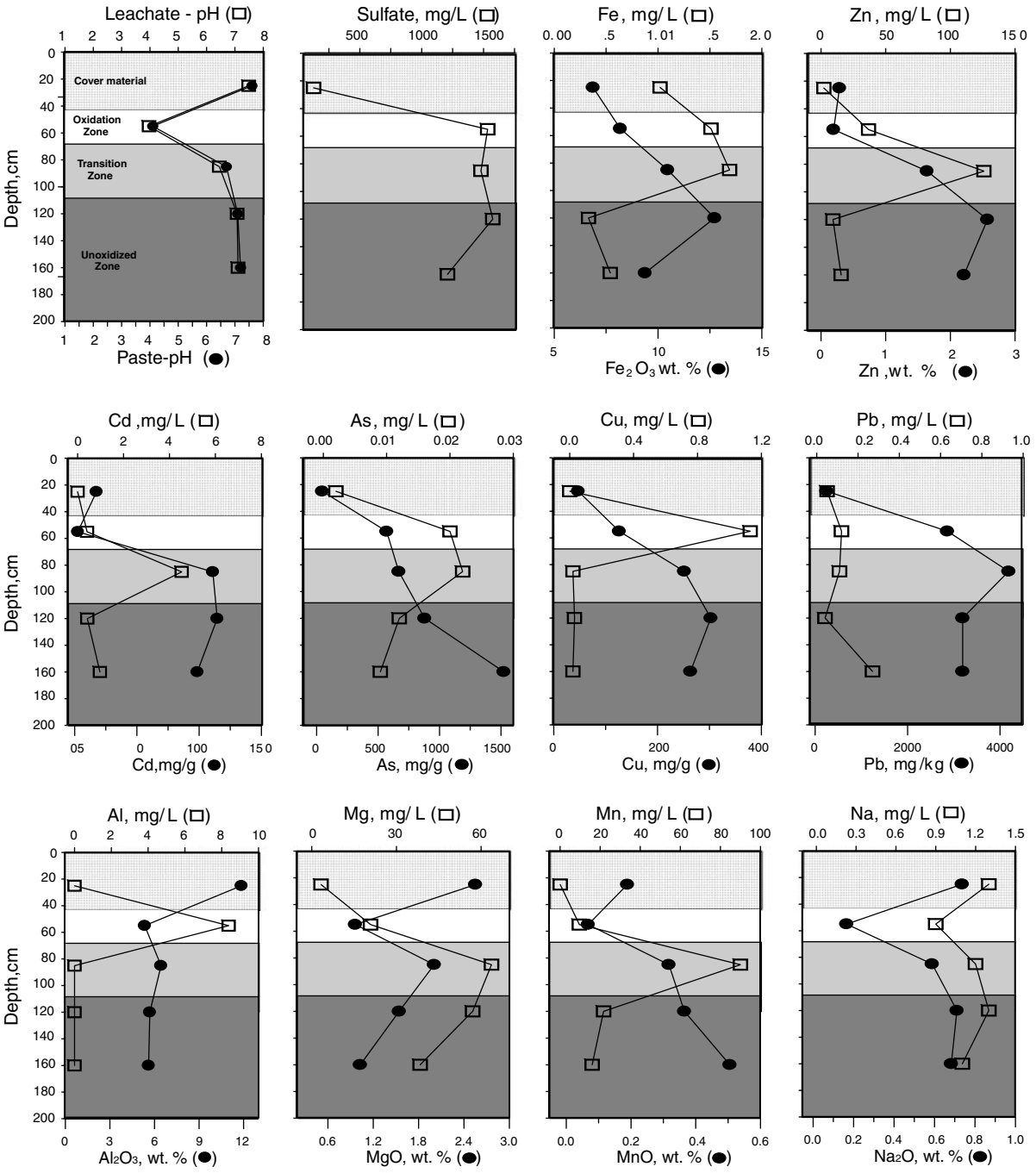

Fig. 5. Chemical composition of tailings solid samples (●) and leachates (□) from representative profile from settling pond.

in the unoxidized tailings, and 5.4 wt.% in the tailings of the transition zone, to an average of 4.1 wt.% in the oxidized tailings. Similarly, Mn concentration decreases from 0.9 to 0.3 wt.%, Mg concentration from 1.2 to 0.5 wt.%, and Na concentration decreases from 1.0 to 0.3 wt.% (Table 2).

4.3. Solid-phase controls on the mobility of sulfide-bound elements in the oxidized zone

The concentration and mobility of dissolved constituents within "El Fraile" tailings are controlled by a complex series of oxidation, precipitation–dissolution and sorption–desorption reactions. The

Table 2
Chemical composition of tailings bulk samples from oxidized, transition and unoxidized zones at "El Fraile" impoundments

Constituent wt.%	Oxidized zone		Transition zone		Unoxidized zone	
	Range	Average ± SD	Range	Average ± SD	Range	Average ± SD
SiO_2	47.9–70.9	59.3 ± 7.4	47.5–62.2	56.6 ± 6.0	41.1–64.4	53.7 ± 9.9
TiO_2	0.2–0.4	0.2 ± 0.1	0.2–0.4	0.3 ± 0.1	0.2–0.4	0.3 ± 0.1
Al_2O_3	2.7–7.1	4.1 ± 1.2	4.3–6.4	5.4 ± 0.8	3.5–6.0	4.7 ± 1.2
CaO	2.0–8.7	5.6 ± 2.2	3.9–5.9	4.9 ± 0.9	3.5–5.2	4.3 ± 0.7
K_2O	1.3–2.2	1.7 ± 0.3	1.4–2.2	1.8 ± 0.3	1.3–2.1	1.7 ± 0.3
Fe_2O_3	5.2–16.5	11.2 ± 3.2	9.7–15.2	11.8 ± 2.1	9.4–23.2	15.6 ± 6.0
MnO	0.1–1.8	0.3 ± 0.5	0.3–1.1	0.7 ± 0.3	0.4–1.5	0.9 ± 0.5
MgO	0.1–1.2	0.5 ± 0.4	1.0–2.0	1.4 ± 0.4	1.0–1.5	1.2 ± 0.3
Na_2O	0.1–0.7	0.3 ± 0.2	0.6–1.0	0.8 ± 0.2	0.6–1.3	1.0 ± 0.3
P_2O_5	0.02–0.10	0.06 ± 0.02	0.05–0.09	0.07 ± 0.02	0.04–0.10	0.07 ± 0.02
LOI	5.2–14.6	9.7 ± 2.6	6.5–11.9	8.5 ± 2.3	5.8–12.9	9.1 ± 3.2
Zn, mg/kg	1300–27,700	6079 ± 7373	4050–20,950	15,800 ± 6769	16,200–32,700	25,267 ± 6168
Pb, mg/kg	1692–5940	3610 ± 1310	1872–4189	2978 ± 1074	1891–3470	2958 ± 554
Cu, mg/kg	83–486	199 ± 118	193–613	334 ± 164	257–501	340 ± 92
As, mg/kg	570–3379	1838 ± 803	668–1542	1323 ± 368	879–1898	1380 ± 338
Cd, mg/kg	2.5–104	33.1 ± 36.7	111–287	181 ± 89	97–384	186 ± 117

Note: LOI, loss on ignition.

concentrations of each dissolved constituent are a function of pH and of the mineralogy of the tailings. The chemistry of aqueous leachates of oxidized tailings indicates that the mobility of SO_4^{2-} and sulfide-bound elements observed in the "El Fraile" tailings follows the sequence $SO_4^{2-} > Fe > Zn > As > Cu > Cd > Pb$.

4.3.1. Sulfate

Oxidation and subsequent dissolution of sulfide minerals, mainly pyrite and sphalerite, is the main source of SO_4^{2-} in the oxidized tailing leachates. However, SO_4^{2-} may also come in the initial sludge since SO_4^{2-} salts are used within the mill process. Sulfate is the dominant anion throughout the tailings leachates. The highest dissolved SO_4^{2-} concentrations were registered in the strongly acidic leachates of the superficial tailings dam (8237–10086 mg L^{-1}) and in the mildly acidic leachates of cemented tailings layers (3715–8541 mg L^{-1}). The lowest concentrations were obtained in the mildly acidic leachates of the settling pond (1534–2047 mg L^{-1}). Geochemical modeling indicates that the oxidized tailings leachates are gypsum oversaturated (SI = 0.1–0.2), and according to the mineralogical study, gypsum and K-jarosite are the most abundant secondary minerals detected within the oxidized tailings. These results indicate that precipitation–dissolution of gypsum and K-jarosite are the major control for the dissolved concentration of SO_4^{2-} within the tailings impoundment, as has been widely reported for similar sites (Johnson et al., 2000; McGregor et al., 1998). Nevertheless, these SO_4^{2-} concentrations partially can be attributed to the dissolution of soluble Cu, Fe and Zn-sulfates, which were not identified probably due to their relatively low abundances.

4.3.2. Iron (Fe)

Oxidation and subsequent dissolution of pyrite is the main source of dissolved Fe in oxidized tailings leachates. The highest dissolved Fe concentrations were registered in the strongly acidic leachates of the superficial tailings dam (2288–2568 mg L^{-1}) and in the mildly acidic leachates of cemented tailings layers (659 mg L^{-1}). However, low concentrations were obtained in the mildly acidic leachates of the tailings settling pond (1.5–5.8 mg L^{-1}).

Pyrite oxidation initially produces Fe-sulfate minerals such as melanterite, the mixed Fe(II)–Fe(III) mineral copiapite and schwermannite (Levy et al., 1997). XRD and microscopic studies showed that the dominant Fe-bearing secondary mineral in

oxidized tailings is K-jarosite (Fig. 6). Besides, according to the MINTEQA2 calculation, the study site's oxidized tailings leachates are oversatured with regard to jarosite (SI = 1.5–11.7), goethite (SI = 1.4–7.2), lepidocrocite (SI = 0.5–6.3) and hematite (SI = 7.8–15.8), and they are below saturation regarding ferryhidrite and ferrous sulfate minerals. This identified mineralogy is consistent with the Eh measured in these samples (ten samples from uncemented layers of oxidized tailings A and B) from 700–800 mV. Jarosite dissolution under the observed conditions (pH < 3) is not favoured, since K-jarosite is a relatively stable secondary mineral under acidic conditions (Baron and Palmer, 1996; McGregor and Blowes, 2002). This suggests that its contribution to the high dissolved Fe and SO_4^{2-} concentration registered in acidic tailings leachates (Table 1) is not important.

Other Fe-bearing secondary minerals detected were goethite (Fig. 7) and lepidocrocite. The solubility diagrams of Fe-oxyhydroxides indicate that under acidic conditions, goethite and

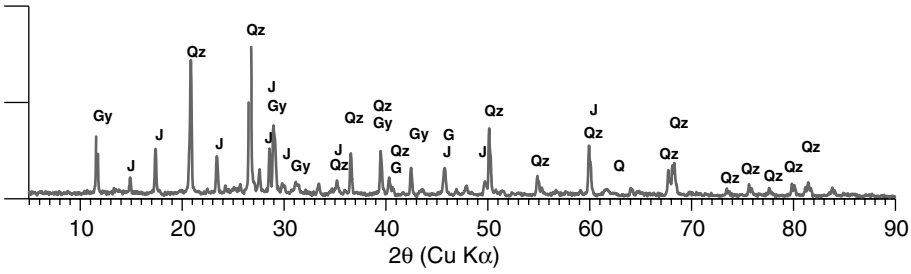

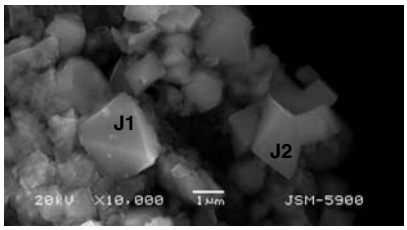

Element	Weight%	
	J1	J2
Al	5.3	4.2
Si	17.7	20.9
S	25.0	24.3
K	8.3	6.5
Fe	34.4	38.3
Zn	7.5	4.8
Cd	1.8	0.9

Fig. 6. SEM-EDS and XRD analysis showing K-jarosite in oxidized tailings. Abbreviations: J, K-jarosite, Q, quartz, Gy, gypsum.

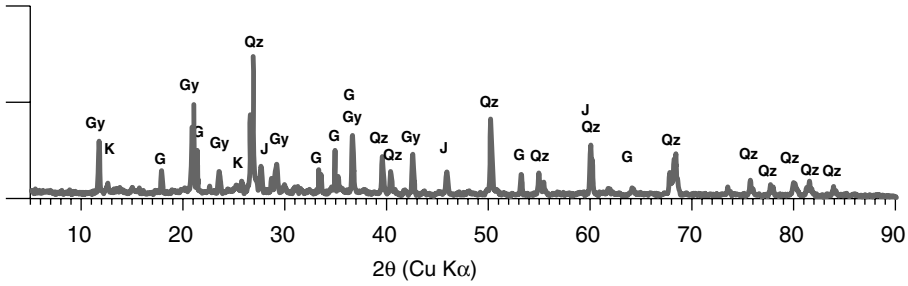

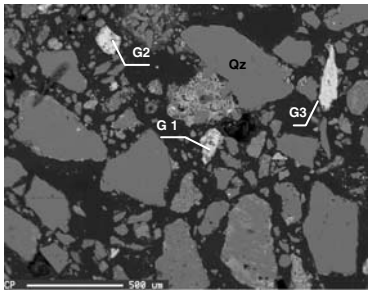

Element	Weight%		
	G1	G2	G3
Na	0.5	0.4	0.7
Al	0.2	0.3	0.6
Si	0.8	1.5	1.1
S	1.6	3.2	2.7
Ca	0.4	0.2	0.2
Fe	95.2	84.2	82.8
Zn	1.9	7.8	6.4
Cd	0.7	0.2	
Cu	0.5	1.1	
As	0.8	1.3	2.7

Fig. 7. SEM-EDS and XRD analysis showing goethite in oxidized tailings. Abbreviations: J, K-jarosite, Q, quartz, Gy, gypsum, G, goethite, K, kaolinite.

lepidocrocite are soluble solid phases and as pH increases their solubility gradually decreases, reaching a minimum between pH 7 and 8 (Cornell and Schwertmann, 1996). Dissolution of Fe-oxyhydroxides is then favoured under acidic and mildly acidic pH conditions and it may be the main source of highly dissolved Fe concentrations registered in acidic and mildly acidic leachates. Nevertheless, dissolved Fe may partially result from dissolution of soluble Fe-sulfates, as mentioned before.

The Fe released in the oxidized acidic tailings dam near the surface (Table 1) is mobile under the prevailing acid conditions and migrated partially downwards through the tailings impoundments. Iron was then removed from leachates, precipitating as goethite, hematite and jarosite at depths where an increase in the pH values of leachates was observed. This mechanism led to the formation of the Fe-cemented layers within "El Fraile" tailings dam, as indicated by the increase of total Fe concentration in the cemented layers. The bulk chemical composition of the oxidized tailings dam indicates that Fe is enriched within the cemented layer with respect to the overlaying oxidized uncemented tailings (Table 3, Fig. 4). The average Fe concentration within cemented layers was 24% greater than the average within the overlying uncemented tailings. Similar Fe-cemented layers have been reported in other inactive tailings deposits (Lin, 1997; McGregor and Blowes, 2002).

4.3.3. Zinc and cadmium

Zinc is released to leachates by oxidation and dissolution of sphalerite that may also contain traces of Cd. The concurrent presence of Cd and zinc suggests that sphalerite oxidation and subsequent dissolution is the primary source of Cd in oxidized tailings leachates. Nevertheless, some Zn may come from the use of Zn-sulfates in the extraction process. The highest dissolved Zn and Cd concentrations were registered in the mildly acidic leachates of cemented tailings layers ($Zn = 645–2435\ mg\ L^{-1}$ and $Cd = 3.6–30.6\ mg\ L^{-1}$) and in the strongly acidic leachates of the superficial tailings dam ($Zn = 107–1309\ mg\ L^{-1}$ and $Cd = 1.1–18.2\ mg\ L^{-1}$). The lowest concentrations were found in the mildly acidic leachates of the tailings settling pond ($Zn = 36.7–50.4\ mg\ L^{-1}$and $Cd = 0.4–0.6\ mg\ L^{-1}$). Mineralogical studies did not detect any secondary Zn and Cd precipitates in oxidized tailings, but SEM-EDS analysis revealed the presence of Zn and Cd traces in K-jarosite (Fig. 6) and Fe-oxyhydroxides grains (Fig. 7) in acid and mildly acid conditions respectively.

These observations suggest that the solid-phase control on the mobility of Zn and Cd, under acidic conditions, appears to be sorption reactions with K-jarosite. However, under mildly acid conditions, the dissolved Zn and Cd concentrations seem to be attenuated by sorption onto Fe-oxyhydroxide grains.

The high concentration of dissolved Zn despite retention by K-jarosite and Fe-oxyhydroxides can

Table 3
Chemical composition of tailings bulk samples from uncemented and cemented layers in the dam's oxidized zone at "El Fraile" impoundments

Constituent wt.%	Uncemented layers		Cemented layers	
	Mean ± SD	Range	Mean ± SD	Range
SiO_2	58.5 ± 5.5	47.9–65.8	55.2 ± 7.8	49.5–66.6
TiO_2	0.2 ± 0.1	0.2–0.4	0.2 ± 0.1	0.2–0.3
Al_2O_3	3.8 ± 1.4	2.7–7.1	4.3 ± 0.9	3.3–5.3
CaO	6.3 ± 1.8	3.5–8.7	5.8 ± 2.1	3.4–8.4
K_2O	1.6 ± 0.2	1.3–1.9	1.6 ± 0.1	1.5–1.7
Fe_2O_3	10.5 ± 2.7	5.2–13.8	13.8 ± 3.8	8.4–16.5
MnO	0.3 ± 0.6	0.1–1.8	0.3 ± 0.1	0.1–0.4
MgO	0.4 ± 0.3	0.1–1.2	0.5 ± 0.3	0.3–0.9
Na_2O	0.3 ± 0.2	0.1–0.7	0.4 ± 0.3	0.1–0.7
P_2O_5	0.04 ± 0.02	0.02–0.07	0.07 ± 0.02	0.05–0.10
LOI	10.3 ± 1.7	7.9–12.3	10.4 ± 3.2	7.0–14.5
Zn, mg/kg	5975 ± 8898	1550–27700	8500 ± 5463	2300–13850
Pb, mg/kg	4369 ± 1203	2693–5940	2626 ± 626	1692–3009
Cu, mg/kg	168 ± 70	83–120	297 ± 170	121–486
As, mg/kg	1556 ± 304	1196–2099	2768 ± 817	1640–3379
Cd, mg/kg	27.4 ± 30.5	8.0–96	59 ± 46	11.0–54

Note: LOI, loss on ignition.

be partially attributed to the dissolution of soluble Zn-sulfates from the flotation process, which were not identified probably due to their relatively low abundances.

Zinc and Cd released from the oxidized acidic tailings dam, near the surface, have partially migrated downwards through the tailings impoundments and were then sorbed onto Fe oxyhydroxides surfaces, as indicated by the enrichment of this element directly above or in the cemented layers (Table 3, Fig. 4). The average Zn and Cd concentrations within these layers were 30% and 54%, respectively, greater than the average concentrations within the overlying uncemented tailings.

4.3.4. Copper (Cu)

Oxidation and dissolution of chalcopyrite is the main source of dissolved Cu concentration. However, small amounts of Cu would also be provided by the initial sludge, due to the use of Cu-sulfate in the process. The highest dissolved Cu contents were registered in the strongly acidic leachates of the superficial tailings dam (15.6–18.3 mg L^{-1}) and in the mildly acidic leachates in layers of cemented tailings (0.5–38.2 mg L^{-1}). Low concentrations were observed in the mildly acidic leachates of the tailings settling pond (1.1–2.2 mg L^{-1}). Calculations with MINTEQA2 indicate that oxidized tailings leachates are undersatured in all discrete Cu-bearing secondary minerals included in the data base. Mineralogical studies did not detect any secondary Cu precipitates in oxidized tailings, but SEM-EDS analysis revealed the presence of traces of Cu in Fe oxyhydroxide grains (Fig. 7). These observations suggest that coprecipitation or adsorption reactions are the dominant solid-phase controls on the mobility of Cu.

Copper released in the oxidized acidic tailings dam near the surface has partially migrated downwards through the tailings impoundments and has then been sorbed onto Fe oxyhydroxides surfaces as indicated by the enrichment of this element directly above or in the cemented layers (Table 3, Fig. 4). The average Cu concentration within these layers was 44% greater than the average within the overlying uncemented tailings.

4.3.5. Lead (Pb)

Oxidation of galena is the primary source of dissolved Pb in the tailings leachates. In contrast to the other heavy metals, which are mobile under acidic conditions, dissolved Pb concentrations were below the detection limits (<0.01 mg L^{-1}) in the superficial oxidized tailings dam, where the leachates are strongly acidic (pH = 1.9–2.0). Nevertheless, in cemented oxidized tailings dam wherein the leachates are mildly acidic (pH = 3.5–4.4), the dissolved Pb concentrations reach a maximum of 0.1–0.6 mg L^{-1}.

Geochemical modeling indicates that the mildly acidic leachates are near satured regarding anglesite (SI = −0.7). SEM-EDS analyses indicate the presence of anglesite in acidic oxidized tailings samples and plumbojarosite in mildly oxidized tailings. Anglesite and plumbojarosite are relatively stable phases under acidic pH conditions, but as pH increases, the dissolution of Pb-sulfates is favored (Roussel et al., 2000). Hence, under the mildly acidic pH conditions that are observed within the cemented tailings dam and uncemented tailings settling pond, the dissolution of Pb-sulfate may contribute to the Pb concentrations registered in these mildly acidic leachates (Table 1).

4.3.6. Arsenic (As)

The occurrence of As with pyrite suggests that its oxidation and subsequent dissolution is the primary source of As in oxidized tailings leachates. Indeed, in the oxidized tailings dam of impoundment "B", where the leachates are strongly acidic (pH = 1.9–2.0), the highest dissolved concentrations of As (101–164 mg L^{-1}) were registered. These high concentrations decrease as pH increases: (i) in oxidized tailings dam leachates of impoundment "A", with a pH from 2.3 to 2.7, the dissolved concentration of As ranges from 0.01 to 4.0 mg L^{-1}, (ii) in the oxidized tailings settling pond, where the leachates are mildly acidic (pH = 2.9–4.0) dissolved concentrations of As range from 0.02 to 0.10 mg L^{-1} and (iii) within cemented tailings leachates, where pH values range from 3.5 to 4.4, the dissolved concentrations of As vary from 0.04 to 0.4 mg L^{-1}. According to the MINTEQA2 calculations, tailings leachates are undersatured regarding all discrete As-bearing secondary minerals included in the database. A mineralogical analysis of oxidized tailings samples did not detect any As-bearing secondary minerals, but SEM-EDS analyses showed that Fe oxyhydroxides contain As traces (Fig. 7). Arsenic contents in grains of Fe-oxyhydroxides analyzed in 15 samples from oxidized tailings varied from 0.2% to 5.2%. These analyses also showed the presence of very small white particles ($\theta < 5$ μm), which contain Fe, Al, S, As, Pb, Zn and Cu in tailings

from cemented layers (Fig. 8). These particles were present everywhere in samples of concentrated oxidized tailings. XRD patterns of these samples revealed peaks that correspond closely to the d-spacing of beudantite (Fig. 9).

These results suggest that the As released is coprecipitated with Fe oxyhydroxides from leachates, or that it is adsorbed after the formation of Fe oxyhydroxides. A change to acidic conditions produces the dissolution of Fe oxyhydroxides and releases As to leachates in the oxidized acidic tailings dam near the surface. Arsenic has partially migrated downwards through the tailings impoundments and has been sorbed onto Fe oxyhydroxide surfaces or precipitated as beudantite in cemented tailings dam. Occurrence of this process is indicated by the enrichment of As directly above or in the cemented layers (Table 3, Fig. 4). The average As concentration within cemented layers was 44% greater than that within the overlying uncemented tailings.

The occurrence of As with Fe oxyhydroxides suggests that removal of As through coprecipitation or adsorption reactions is most likely, the dominant solid-phase control on the mobility of As in these oxidized tailings. Besides, the identification of beudantite in cemented layers indicates that precipitation of this mineral is another important control in the mobility of As under mildly acidic conditions within cemented tailings. The identification and significance of the occurrence of beudantite within "El Fraile" oxidized tailings will be discussed next.

4.3.7. Identification and significance of Beudantite

Beudantite, an As and Pb-containing species structurally related to the alunite–jarosite family of minerals, is characterized by roughly equal proportions of As and S instead of S only as well as by the predominance of Fe rather than Al as the trivalent cation (Szymanski, 1988). Certain identification of beudantite within the "El Fraile" tailings is significant because several authors have reported that it plays an important role in the natural attenuation of As and Pb in sulfide oxidation processes. Beudantite has been reported as a natural mechanism of As and Pb fixation in superficial sulfide deposits (Nieto et al., 2003). In La Petite Faye tailings in France, beudantite ensured an efficient trapping of As and Pb in Au-mine tailings (Courtin-Nomade et al., 2002; Roussel et al., 2000). The accumulation of As in a jarosite-beudantite solid solution at Berikul Au mine (Siberia, Russia) has also been reported (Giere et al., 2003).

Roussel et al. (2000) identified the presence of beudantite using SEM-EDS and X-RD methods. However, considering the similarity of XRD patterns ("*d*" values/Å intensity %) for beudantite (3.07/100, 5.94/74.7, 3.66/40.4, 1.98/26.8, 2.27/24.7, 1.83/20.16, 2.97/17.3, 2.31/8.4) and those for

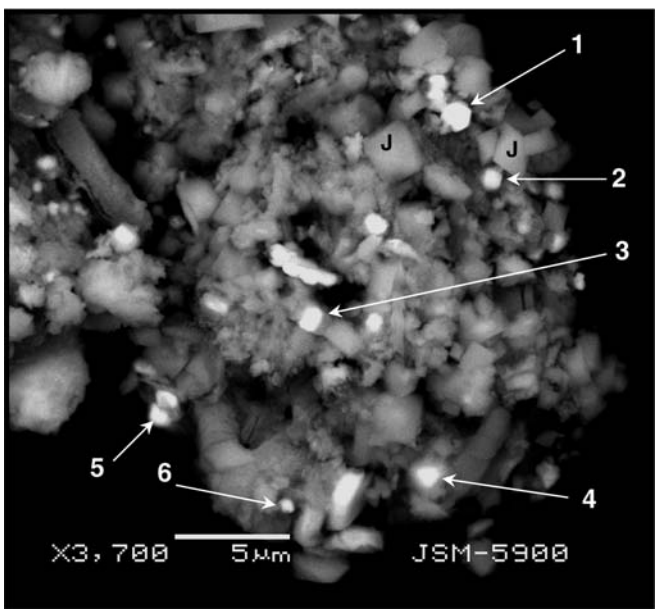

Fig. 8. SEM (backscattered electron) of the concentrated (<40 μm) oxidized tailings sample from cemented layers showing K-jarosite grain (J) and small white particles (1, 2, 3, 4, 5 and 6) which contain Fe, S, As, Pb, Zn and Cu.

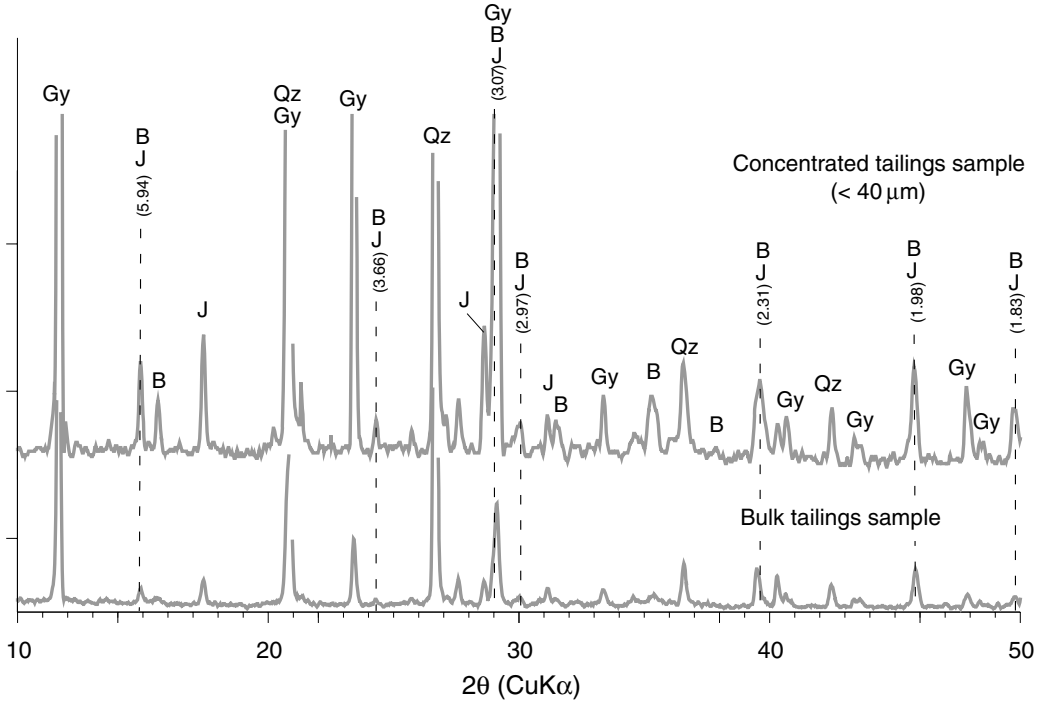

Fig. 9. XRD patterns of bulk and concentrated sample of cemented layer from oxidized tailings dam. The position of the similar peaks of beudantite and K-jarosite is shown with the dashed lines at 5.94 Å, 3.66 Å, 3.07 Å, 2.97 Å, 2.31 Å, 1.98 Å, and 1.83 Å. Abbreviations: B, beudantite, J, K-jarosite, Q, quartz, Gy, gypsum.

K-jarosite (3.08/100, 3.11/63.7, 5.10/55.9, 5.94/36.7, 1.98/33.3, 2.30/31.9, 2.97/14.9, 3.66/12.2), the identification of beudantite in tailings samples is extremely difficult using only these two methods.

The presence of beudantite detected by SEM-EDS and XRD in concentrated oxidized tailings samples (<40 μm fractions) of the "El Fraile" impoundments was verified in this work using transmission electron microscopy (TEM) with energy dispersive spectrometry (EDS). Fig. 10 shows TEM images and energy dispersive spectra (EDS) for small white grains of oxidized tailings. Crystallographic "d" values calculated from the selected-area electron diffraction pattern (Fig. 10b) conform with those of beudantite. EDS analyses (Fig. 10c) indicate that the chemical composition is also consistent with the occurrence of beudantite. Besides, EDS showed the presence of Zn and Cu, possibly coprecipitated in beudantite crystals. The high-resolution image showing regular lattice fringes (Fig. 10d) and the obtained electron diffraction pattern (Fig. 10b) show the crystalline character and rhombohedral crystal system of beudantite (Szymanski, 1988).

There may be two possible mechanisms for the formation of beundantite ($PbFe_3(AsO_4)(SO_4)(OH)_6$) within "El Fraile" tailings. One is the replacement of SO_4^{2-} groups by AsO_4^{3-} in detected plumbojarosite. Similar anionic substitution has been reported in roasted sulfide ore from the Spenceville Mine, wherein AsO_4^{3-} replaced SO_4^{2-} groups in K-jarosite (Foster et al., 1998). An alternative mechanism is direct precipitation, through the combination of As, Fe, Pb and S released by dissolution and desorption reactions of the respective solid phases that take place in the cemented layers under mildly acidic pH conditions.

Few data have been reported on the solubility of beudantite. Roussel et al. (2000) estimated a value from 10^{-15} to 10^{-21} for the solubility constant of beudantite, at 298 °K, using the standard Gibbs energy of formation of plumbojarosite of -727.5 kcal mol^{-1}, which is very similar to the predicted Gibbs energy of formation of beudantite (Gaboreau and Vieillard, 2004). These values indicate the low solubility of beudantite. In the cemented tailings dam of the "El Fraile" impoundment, where beudantite appears to be one of the solid phase controlling the mobility of As, the concentration of dissolved As is up to one order of magnitude greater in impoundment "B" ($As = 0.4$ mg L^{-1})

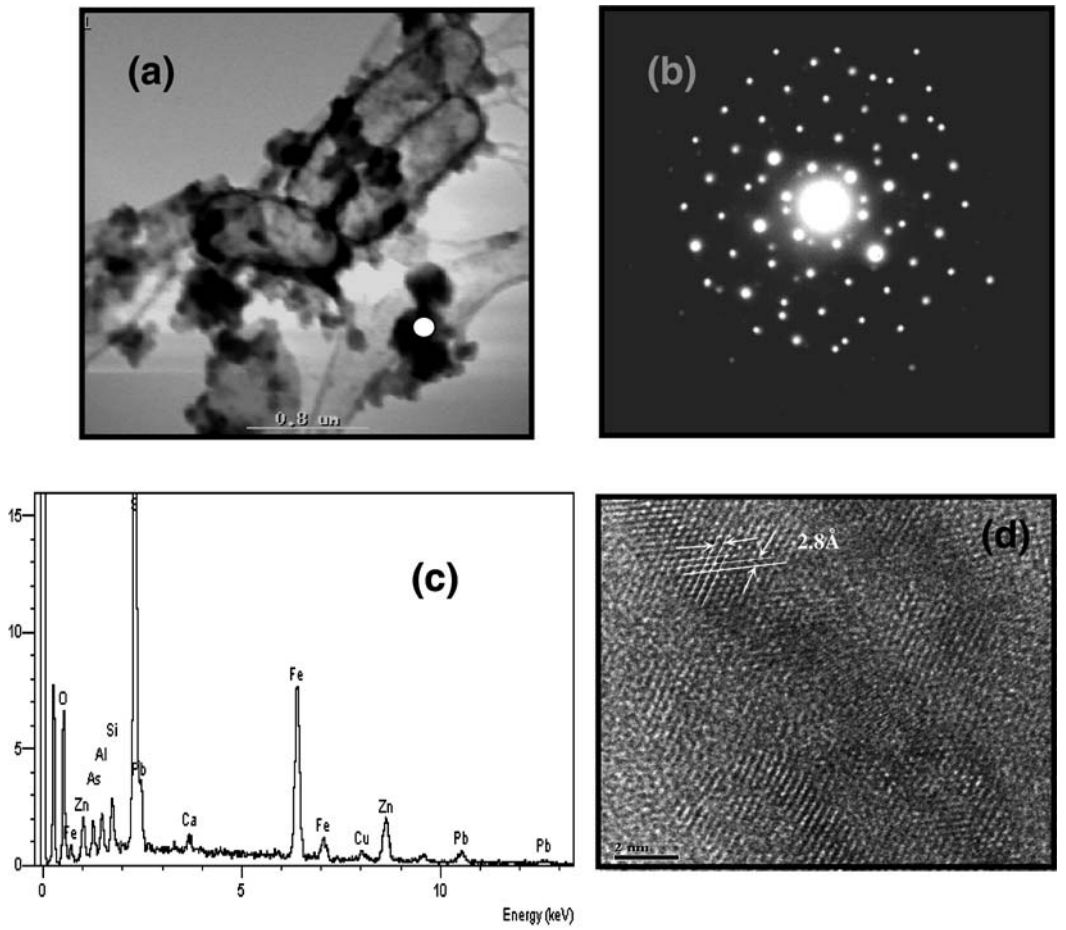

Fig. 10. TEM images of concentrated tailings sample from cemented tailings dam. (a) White dots show location of energy-dispersive analyses (EDS). (b) Electron diffraction pattern. (c) EDS spectra and (d) High-resolution image.

than in impoundment "A" (As from 0.04 to 0.10 mg L^{-1}) (Table 1). These values suggest differences between the solubility of beudantite present in the cemented layers of each tailings impoundment. The apparent difference in beundantite's solubility could be explained by the presence of other elements incorporated into the mineral structure.

The SEM-EDS analyses showed different contents of Zn and Cu in beundantite particles in samples from each impoundment. Beudantite grains in tailings sampled from cemented layers of impoundment "*A*" contain approximately 5–18% Zn and 2–3% Cu. However, beudantite grains in tailings sampled from similar layers of impoundment "*B*" contain 1–5% Zn and they do not contain Cu. These results suggest that the formation of beudantite, in the presence of dissolved Zn and Cu results in a significant co-precipitation of these metals in the beudantite phase; the co-precipitation was more pronounced in cemented tailings dam at impoundment "*A*", than at impoundment "*B*". These observations indicate that the incorporation of significant Zn and Cu into the structure of beudantite in the cemented tailings dam at impoundment "*A*" may be the cause of the low solubility of beudantite in these tailings and consequently, of the lower dissolved concentration of As in the leachates. However, the role of coprecipitated Cu and Zn on the solubility of beudantite, has to be studied further to better support the above considerations. It is thus necessary to conduct experiments with synthetic beudantite and variable concentrations of Cu and Zn.

5. Conclusions

Sulfide oxidation reactions in the "El Fraile" tailings impoundment have produced low pH conditions

in the oxidized zone and high concentrations of water-leachable heavy metals, As and SO_4^{2-}. The oxidation process has been less extensive in the settling pond than in the dam and the oxidation front has consequently penetrated down to depths of approximately 60–100 cm in the dam, and only 20 cm in the settling pond.

The leachate pH values and concentrations of dissolved constituents form a stepwise profile in the tailings, with noticeable differences between the dam and the settling pond: (i) in the tailings dam, the low pH values (pH = 1.9–2.7) of the leachates in the uppermost parts of the oxidized zone indicate the readily available acidity in the active oxidation zone. These low pH values rise gradually with depth (pH = 3.5–4.4) indicating that the generated H^+ ions are consumed by dissolution of the identified aluminosilicate minerals. This pH rise causes the precipitation of Fe oxyhydroxides, forming the cemented layers in the dam from "El Fraile" tailings. These layers have restricted the oxidizing agent's diffusion through the tailings and this, in turn, has restricted the transport of dissolved constituents downwards through the tailings dam. Below the cemented layer, where weakly altered and unoxidized tailings occur, the pH increases abruptly to near neutral (pH = 6.4–6.9) and soluble concentrations of most metals and SO_4^{2-} decrease. (ii) the leachate pH values in the oxidized zone of the settling pond (pH = 2.9–4.0) are higher than those registered in leachates of superficial oxidized tailings dam, consequently soluble concentrations of constituents are lower. These pH values increase to near neutral (pH = 6.5) with depth, where the weakly altered and unoxidized tailings occur. Nevertheless, the absence of a cemented layer in the oxidized zone of the settling pond has allowed the transport of dissolved constituents downwards through the tailings.

The concentration and mobility of potentially toxic elements (PTE) are controlled by a series of precipitation and sorption reactions. The main controls on the mobility of PTE within the "El Fraile" tailings impoundments appear to be sorption and desorption reactions on Fe-precipitates. The very low dissolved concentration of Pb in acidic leachates may be attributed to precipitation of plumbojarosite and anglesite that are relatively stable phases under acidic pH conditions, but as pH increases, dissolution of Pb-sulfates may contribute to dissolved Pb in mildly acidic leachates. Additionally, it was observed that As and Pb in mildly acidic leachates from cemented layers were effectively removed by the precipitation of beudantite and had been naturally attenuated. Beundantite's solubility appears to be retarded by the incorporation of significant Zn and Cu in the structure; attenuation of As and Pb by beudantite is thus expected to be maintained over a long term in these Zn and Cu rich tailings.

Acknowledgements

We express our gratitude to Industrial Minera México (IMMSA) for their interest, access to the properties, their financial and logistic support and their collaboration, especially that of V.Muhech – Dip, R. Rubio, J.J. López, F. Wong, H. Solís and R. Cordero. We sincerely thank Kathleen Smith and Peter Swedlund for their reviews and comments that greatly improved this paper. We are grateful to I. Puente Lee (Facultad de Química, UNAM) and C. Briseño (Instituto de Geofísica, UNAM), for technical aid in electron microscope measurements. We also thank J.C. Cruz (Facultad de Ingeniería, UNAM) for aid in optical microscopy analyses. Our acknowledgements to C. Salcedo (Facultad de Química, UNAM) and R. Lozano (Instituto de Geología, UNAM) for XRD and XRF analyses. Thanks also to O. Cruz, N. Ceniceros and A. Aguayo (Instituto de Geofísica, UNAM) for assistance in laboratory work. CONACYT-SEMARNAT project C01-0017-2002 is acknowledged for funding.

References

Allison, J.D., Brown, D.S., Novogradac, K.J., 1991. MINTEQA2/PRODEFA2, A Geochemical Assesment Model for Enviromental Systems: version 3.11 Users Manual. EPA/600/3-91/021, Washington, DC. USA.

Armienta, M.A., Villaseñor, G., Rodriguez, R., Ongley, L.K., Mango, H., 2001. The role of arsenic-bearing rocks in groundwater pollution at Zimapan Valley, Mexico. Environ. Geol. 40, 571–581.

Bain, J.G., Blowes, D.W., Robertson, W.D., Frind, E.O., 2000. Modelling of sulfide oxidation with reactive transport at a mine drainage site. J. Contam. Hydrol. 41, 23–47.

Balistrieri, L.S., Box, S.E., Bookstrom, A.A., Ikramuddin, M., 1999. Assessing the influence of reacting pyrite and carbonate minerals on the geochemistry of drainage in the Coeur d'Alene mining district. Environ. Sci. Technol. 33, 3347–3353.

Baron, D., Palmer, C.D., 1996. Solubility of jarosite at 4–35 °C. Geochim. Cosmochim. Acta 60, 185–195.

Blowes, D.W., R.E., Jambor JL, Cherry JA, 1991. The formation and potential importance of cemented layers in inactive sulfide mine tailings. Geochim. Cosmochim. Acta 55, pp. 965–978.

Blowes, D.W., Jambor, J.L., Hanton-Fong, C.J., Lortie, L., Gould, W.D., 1998. Geochemical, mineralogical and microbiological characterization of a sulphide-bearing carbonate-rich gold-mine tailings impoundment, Joutel, Quebec. Appl. Geochem. 13, 687–705.

Cornell, R., Schwertmann, U., 1996. The Iron Oxides: Structure, Properties, Reactions, Occurrence and Uses. VCH Publisher, New York.

Courtin-Nomade, A., Bril, H., Neel, C., Lenain, J.F., 2003. Arsenic in iron cements developed within tailings of a former metalliferous mine – Enguiales, Aveyron, France. Appl. Geochem. 18, 395–408.

Courtin-Nomade, A., Neel, C., Bril, H., Davranche, M., 2002. Trapping and mobilisation of arsenic and lead in former mine tailings – Environmental conditions effects. Bull. Soc. Geol. France 173, 479–485.

Dold, B., Fontbote, L., 2001. Element cycling and secondary mineralogy in porphyry copper tailings as a function of climate, primary mineralogy, and mineral processing. J. Geochem. Explor. 74, 3–55.

Foster, A.L., Brown, G.E., Tingle, T.N., Parks, G.A., 1998. Quantitative arsenic speciation in mine tailings using X-ray absorption spectroscopy. Am. Mineral. 83, 553–568.

Fukushi, K., Sasaki, M., Sato, T., Yanase, N., Amano, H., Ikeda, H., 2003. A natural attenuation of arsenic in drainage from an abandoned arsenic mine dump. Appl. Geochem. 18, 1267–1278.

Gaboreau, S., Vieillard, P., 2004. Prediction of Gibbs free energies of formation of minerals of the alunite supergroup. Geochim. Cosmochim. Acta 68, 3307–3316.

Giere, R., Sidenko, N.V., Lazareva, E.V., 2003. The role of secondary minerals in controlling the migration of arsenic and metals from high-sulfide wastes (Berikul gold mine, Siberia). Appl. Geochem. 18, 1347–1359.

Holmstrom, H., Ohlander, B., 2001. Layers rich in Fe- and Mn-oxyhydroxides formed at the tailings-pond water interface, a possible trap for trace metals in flooded mine tailings. J. Geochem. Explor. 74, 189–203.

Holmstrom, H., Salmon, U.J., Carlsson, E., Petrov, P., Ohlander, B., 2001. Geochemical investigations of sulfide-bearing tailings at Kristineberg, northern Sweden, a few years after remediation. Sci. Total Environ. 273, 111–133.

IMMSA (Industrial Minera México S.A.), 1973. Yacimientos minerales metálicos del Distrito Minero de Taxco, Reporte Interno, Taxco, Guerrero-México.

IMMSA (Industrial Minera México S.A.), 1980. Estimación de reservas en los jales inactivos de Taxco, Reporte Interno, Taxco, Guerrero-México.

INEGI, 1999. Síntesis geográfica del Edo. De Hidalgo. Instituto Nacional de Estadística, Geografía e Informática, Aguascalientes, México.

Johnson, R.H., Blowes, D.W., Robertson, W.D., Jambor, J.L., 2000. The hydrogeochemistry of the Nickel Rim mine tailings impoundment, Sudbury, Ontario. J. Contam. Hydrol. 41, 49–80.

Jung, M.C., 2001. Heavy metal contamination of soils and waters in and around the Imcheon Au–Ag mine, Korea. Appl. Geochem. 16, 1369–1375.

Levy, D.B., Custis, K.H., Casey, W.H., Rock, P.A., 1997. A comparison of metal attenuation in mine residue and overburden material from an abandoned copper mine. Appl. Geochem. 12, 203–211.

Lin, Z., 1997. Mobilization and retention of heavy metals in mill-tailings from Garpenberg sulfide mines, Sweden. Sci. Total Environ. 198, 13–31.

Ljungberg, J., Ohlander, B., 2001. The geochemical dynamics of oxidising mine tailings at Laver, Northern Sweden. J. Geochem. Explor. 74, 57–72.

Martycak, K., Zeman, J., Vacek-Vesely, M., 1994. Supergene processes on ore deposits-a source of heavy metals. Environ. Geol. 23, 156–165.

McGregor, R.G., Blowes, D.W., 2002. The physical, chemical and mineralogical properties of three cemented layers within sulfide-bearing mine tailings. J. Geochem. Explor. 76, 195–207.

McGregor, R.G., Blowes, D.W., Jambor, J.L., Robertson, W.D., 1998. The solid-phase controls on the mobility of heavy metals at the Copper Cliff tailings area, Sudbury, Ontario, Canada. J. Contam. Hydrol. 33, 247–271.

Moncur, M.C., Ptacek, C.J., Blowes, D.W., Jambor, J.L., 2005. Release, transport and attenuation of metals from an old tailings impoundment. Appl. Geochem. 20, 639–659.

Nieto, J.M., Capitan, M.A., Saez, R., Almodovar, G.R., 2003. Beudantite: a natural sink for As and Pb in sulphide oxidation processes. Appl. Earth Sci. 112, B293–B296.

Paktunc, D., Foster, A., Heald, S., Laflamme, G., 2004. Speciation and characterization of arsenic in gold ores and cyanidation tailings using X-ray absorption spectroscopy. Geochim. Cosmochim. Acta 68, 969–983.

Roussel, C., Neel, C., Bril, H., 2000. Minerals controlling arsenic and lead solubility in an abandoned gold mine tailings. Sci. Total Environ. 263, 209–219.

Savage, K.S., Tingle, T.N., O'Day, P.A., Waychunas, G.A., Bird, D.K., 2000. Arsenic speciation in pyrite and secondary weathering phases, Mother Lode Gold District, Tuolumne County, California. Appl. Geochem. 15, 1219–1244.

Szymanski, J., 1988. The crystal structure of beudantite, $Pb(Fe,Al)_3[(As,S)O_4]_2(OH)_6$. Can. Mineral. 26, 923–932.

USEPA, 1994. Microwave Assisted Acid Disgestion/sludges, soils. <http://www.epa.gov/epaoswer/hazwaste/test/main.htm>.

USEPA, 1996. Inductively Coupled Plasma Atomic Emission Spectroscopy. <http://www.epa.gov/epaoswer/hazwaste/test/main.htm>.